Technical Review

No.1 – 1994

Digital Filter Techniques vs. FFT Techniques for Damping Measurements

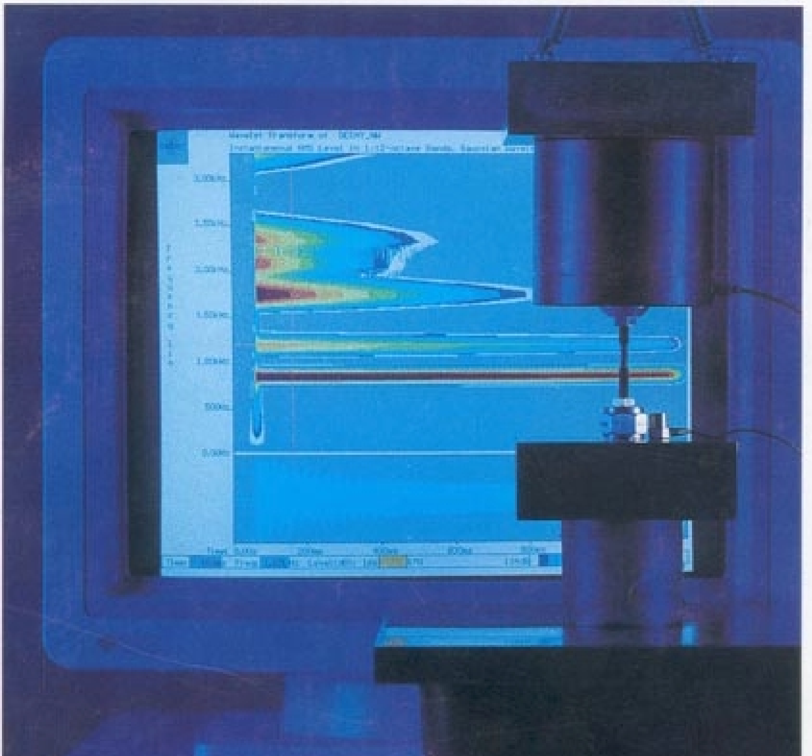

Brüel & Kjær

Previously issued numbers of Brüel & Kjær Technical Review

(Continued on cover page 3)

Technical Review

No. 1 -1994

Contents

Editor: K. Zaveri Photographer: Peder Dalmo
Layout: Judith Sarup Printed by Nærum Offset

Digital Filter Techniques vs. FFT Techniques for Damping Measurements (Damping Part I)

by Svend Gade & Henrik Herlufsen

Abstract

In this article several methods for measurements of damping are summarized with respect to their advantages and disadvantages. Especially the use of Digital Filters (DF) and Fast Fourier Transform (FFT) are compared. In general FFT analysis is best suited for heavily damped structures although with proper memory and postprocessing facilities, lightly damped structures may also be covered, while it is advantageous to use DF analysis when dealing with lightly damped structures only. The use of Time-frequency analysis techniques such as the Wavelet Transform and the Short-time Fourier Transform is also demonstrated.

Resume

Cet article décrit succintement les avantages et les inconvénients respectifs de plusieurs méthodes utilisées pour les mesures d'amortissement. Y sont spécialement comparées la méthode par filtrage numérique (DF) et la méthode par Transformée de Fourier rapide (FFT). Si l'analyse FFT convient généralement mieux pour les structures fortement amorties, bien que, avec mémoire et post-traitement appropriés, elle puisse également s'appliquer pour les structures légèrement amorties, l'analyse DF est, elle, particulièrement adéquate lorsque seules les structures légèrement amorties sont à mesurer. L'utilisation de techniques d'analyse en fréquence dans le domaine temporel, telles que la Transformée d'ondelettes et la Transformée de Fourier courte durée y est égaleemnt traitée.

Zusammenfassung

Dieser Artikel stellt die Vor- mid Nachteile für mehrere Methoden der Dämpfungsmessung einander gegenüber. Insbesondere werden die Digitalfilter-Technik (DF) und die Fast Fourier Transformation (FFT) miteinander verglichen. Im allgemeinen eignet sich die FFT-Analyse am besten für stark gedämpfte Strukturen, wobei mit geeigneten Speicher- und Nachbearbeitungsfunktionen auch die Analyse schwach gedämpfter Strukturen möglich ist. DF-Analyse ist vorteilhaft, wenn ausschließlich schwach gedämpfte Strukturen zu untersuchen sind. Die Anwendung von Zeit/Frequenz-Analysetechniken wie Wavelet-Transformation und Kurzzeit-Fourier-Transformation wird ebenfalls diskutiert.

Nomenclature

a	wavelet scaling factor
b	time parameter
c	viscous damping coefficient
c_c	critical damping coefficient
dB	decibels, ten times the logarithm to a (power) ratio
e	base of natural logarithm, 2,72...
f	frequency [Hz]
f_o	undamped natural frequency [Hz]
fd	modal damping frequency [Hz]
g	grammes, time weighting function
m	milli, 10^{-3}
min	minutes
s	seconds
sec	seconds
A, A_o, A_{ref}	constants, amplitudes
B&K	Brüel&Kjær
C_o	constant, initial value
D	decay rate [dB/s]
DF	digital filters
DFT	discrete fourier transform
E	total energy [J]
FFT	Fast Fourier Transform
FRF	Frequency response function
$H_1(f)$	estimator of frequency response function

$H_2(f)$	estimator of frequency response function
Hz	hertz [s^{-1}]
IRF	Impulse response function
J	joules
MDOF	Multiple Degree of Freedom
P	input power [W]
Q	quality factor, gain factor
s	time signal
S	Frequency Spectrum
SDOF	Single Degree of Freedom
SMS	Structural Measurement System
STAS	Structural Testing and Analysis System
STFT	Short-time Fourier Transform
T	FFT record length
T_A	averaging time
T_{60}	reverberation time [s]
W	watts
W_s	Wigner-Ville distribution
WVD	Wigner-Ville distribution
WT	Wavelet Transform
^	estimated value
δ	the logarithm decrement
ζ	fraction of critical damping, damping ratio
ζ_ω	damping ratio of exponential weighting function
η	loss factor
π	pi 3.14.....
ψ	Wavelet
σ	decay constant [s^{-1}]
σ	modal damping frequency [Rad/s]
τ	time constant [s], time shift
τ_s	time constant of structure [s]
τ_d	time constant of exponential detector [s]
τ_w	time constant (length) of exponential weighting function [s]
ω	angular frequency [Rad/s]
ω_d	damped natural frequency [Rad/s]
ω_o	undamped natural frequency [Rad/s]
Δf	3 dB bandwidth [Hz]
ΔF	FFT line spacing [Hz]
$\Delta\omega$	3 dB bandwidth [Rad/s]

%	per cent, 10^{2-}
⟨⟩	inner products
*	complex conjugate

Introduction

One of the modal parameters is the damping. Without any doubt this quantity is very important to know for the design and analysis of vibrating structures. For example the predicted response due to a simulated input requires an accurate knowledge of the damping properties. The damping of combined and complex structures is often dominated by losses at joints etc. and thus is very difficult to model and predict analytically. In general, the damping of materials and structures must be determined experimentally i.e. measured.

Many different methods exist for the measurement of damping. These can roughly be divided into three groups namely

1) Vibration decay measurements
2) Bandwidth determination of measured modal resonances
3) Steady-state measurements of input and stored energy

This article will not deal with steady-state technique which is based on the energy balance in structures that are vibrationally excited (see Ref.[1]). In the steady-state techniques the input power flow, *P is* estimated from the time-averaged product of force and velocity at the driving point, and the total stored energy, *E* is determined as twice the kinetic energy, which is estimated by integrating the product of mass density and squared velocity over the structure. Then the loss factor, η is determined from the relation $\eta = P/\omega E$. Using this method damping can in theory be estimated even in frequency bands without resonance frequencies.

In this paper the use of *Digital Filter* (DF) techniques and *Discrete Fourier Transform* (DFT/FFT) techniques are compared. A DF analyzer gives a real-time constant percentage bandwidth analysis i.e. 1/1 octaves, 1/3 octaves, 1/12 octaves and 1/24 octaves which are respectively 70%, 23%, 6% and 3% analysis, while an DFT/FFT analyzer gives a blockwise constant bandwidth (narrow band) analysis. The use of Time-frequency analysis techniques such as the Wavelet transform and the Short-time Fourier Transform is also demonstrated.

There exist of course several other methods than those described in this paper. For example in Ref.[11] it is shown how to measure damping via probability functions.

Damping Descriptors

There exist several damping descriptors, e.g. loss factor, quality factor, reverberation time etc. The interrelation between some of these descriptors are summarized in Table 1. The explanation why there exists so many damping descriptors is mainly due to historical reasons and the different fields of applications. For modal damping based on frequency response functions it is quite natural to measure the 3dB bandwidth $\Delta\omega$, Δf while for free decay measurements one will normally measure decay rate, *D,* time constants, τ or reverberation time, T_{60}. In room acoustics the reverberation time (i.e. the time it takes the signal level to decrease 60 dB after the signal source has been switched off) is exclusively used due to specifications as found in international standards, while in mechanics the decay rate, *D* is preferred (Ref. [8]). The logarithmic decrement, δ is very seldom used nowadays. This descriptor is defined as the logarithm of the amplitude ratio of successive maxima, normally observed using an oscilloscope and provided that only one resonance is present.

In modal analysis the decay constant, σ (or modal damping frequency in [Rad/s]) is often used since $-\sigma$ indicates the real part of the pole location of transfer functions in the Laplace plane. On decay curves the decay constant, σ corresponds to the number of -8.7dBs the curve decays per second (i.e. the number of time constants, τ, per second).

For material testing damping is often expressed as a relative thus dimensionless quantity such as loss factor, η, fraction of critical damping, ζ or quality factor, *Q*.

The original definition of loss factor for non-resonant materials is taken as the ratio between the quadrature and coincident part of the complex modulus, which is relating stress and strain in a material. The loss factor indicates what fraction of the vibratory mechanical energy that is lost (i.e., converted into heat) in one cycle of vibration (see for example, Refs. [6] and [7]).

The quality (or gain) factor is often used in the field of electronics to describe the properties of resonators and filters.

The fraction of critical damping which only differs from the loss factor by a factor of 2 is used in the field of modal analysis and expresses the ratio between the modal damping frequency σ and the undamped natural frequency ω_o, i.e. the unsigned ratio between the real part and the distance from the origin of the pole location of transfer functions in the complex Laplace plane. It can be shown that using a viscously damped single degree of freedom model consisting of a mass, a spring and a viscous dashpot, c that the fraction of critical damping (often also called the damping ratio) equals the ratio between the actual damping, c and damping there would have been, c_c if the system was

Natural Frequency $\omega_0 = 2\pi f_o$ (= ω_d for lightly damped resonances)											
Unknown / Known	$\Delta\omega=$	$\Delta f=$	$f_d=$	$\eta=$	$\zeta=$	$Q=$	$\sigma=$	$\tau=$	$T_{60}=$	$D=$	$\delta=$
3dB Bandwidth $\Delta\omega$ [Rad/s]	$\Delta\omega$	$\frac{\Delta\omega}{2\pi}$	$\frac{\Delta\omega}{4\pi}$	$\frac{\Delta\omega}{\omega_o}$	$\frac{\Delta\omega}{2\omega_o}$	$\frac{\omega_o}{\Delta\omega}$	$\frac{\Delta\omega}{2}$	$\frac{2}{\Delta\omega}$	$\frac{13.8}{\Delta\omega}$	$4.34\Delta\omega$	$\frac{\pi\Delta\omega}{\omega_o}$
3dB Bandwidth Δf [Hz]	$2\pi\Delta f$	Δf	$\frac{\Delta f}{2}$	$\frac{\Delta f}{f_o}$	$\frac{\Delta f}{2f_o}$	$\frac{f_o}{\Delta f}$	$\pi\Delta f$	$\frac{1}{\pi\Delta f}$	$\frac{6.9}{\pi\Delta f}$	$27.3\Delta f$	$\frac{\pi\Delta f}{f_o}$
Damping frequency f_d [Hz}	$4\pi f_d$	$2f_d$	f_d	$\frac{2f_d}{f_o}$	$\frac{f_d}{f_o}$	$\frac{f_o}{2f_d}$	$2\pi f_d$	$\frac{1}{2\pi f_d}$	$\frac{1.1}{f_d}$	$54.6f_d$	$\frac{2\pi f_d}{f_o}$
Loss Factor η	$\eta\omega_o$	ηf_o	$\frac{\eta f_o}{2}$	η	$\frac{\eta}{2}$	$\frac{1}{\eta}$	$\eta\pi f_o$	$\frac{1}{\pi f_o\eta}$	$\frac{2.2}{\eta f_o}$	$4.34\omega_o\eta$	$\eta\pi$
Fraction of critical damping ζ	$2\zeta\omega_o$	$2\zeta f_o$	$2\zeta f_o$	2ζ	ζ	$\frac{1}{2\zeta}$	$2\pi f_o\zeta$	$\frac{1}{2\pi f_o\zeta}$	$\frac{1.1}{\zeta f_o}$	$8.69\omega_o\zeta$	$2\pi\zeta$
Quality factor Q	$\frac{\omega_o}{Q}$	$\frac{f_o}{Q}$	$\frac{f_o}{2Q}$	$\frac{1}{Q}$	$\frac{1}{2Q}$	Q	$\frac{\omega_o}{2Q}$	$\frac{2Q}{\omega_o}$	$\frac{22Q}{f_o}$	$\frac{4.34\omega_o}{Q}$	$\frac{\pi}{Q}$
Decay constant σ [s^{-1}]	2σ	$\frac{\sigma}{\pi}$	$\frac{\sigma}{2\pi}$	$\frac{2\sigma}{\omega_o}$	$\frac{\sigma}{\omega_o}$	$\frac{\omega_o}{2\sigma}$	σ	$\frac{1}{\sigma}$	$\frac{6.9}{\sigma}$	8.69σ	$\frac{\sigma}{f_o}$
Time constant τ [s]	$\frac{2}{\tau}$	$\frac{1}{\pi\tau}$	$\frac{1}{2\pi\tau}$	$\frac{1}{\pi f_o\tau}$	$\frac{1}{2\pi f_o\tau}$	$\pi f_o\tau$	$\frac{1}{\tau}$	τ	6.9τ	$\frac{8.69}{\tau}$	$\frac{1}{f_o\tau}$
Reverberation time T_{60} [s]	$\frac{13.8}{T_{60}}$	$\frac{2.2}{T_{60}}$	$\frac{1.1}{f_oT_{60}}$	$\frac{2.2}{f_oT_{60}}$	$\frac{1.1}{f_oT_{60}}$	$\frac{f_oT_0}{2.2}$	$\frac{6.9}{T_{60}}$	$\frac{T_{60}}{6.9}$	T_{60}	$\frac{60}{T_{60}}$	$\frac{6.9}{f_oT_{60}}$
Decay rate D [dB/s]	$\frac{D}{4.34}$	$\frac{D}{27.3}$	$\frac{D}{54.6}$	$\frac{D}{4.34\omega_o}$	$\frac{D}{8.69\omega_o}$	$\frac{4.34\omega_o}{D}$	$\frac{D}{8.69}$	$\frac{8.69}{D}$	$\frac{60}{D}$	D	$\frac{D}{8.69f_o}$
The logarithmic decrement δ	$\frac{\delta\omega_o}{\pi}$	$\frac{\delta f_o}{\pi}$	$\frac{\delta f_o}{2\pi}$	$\frac{\delta}{\pi}$	$\frac{\delta}{2\pi}$	$\frac{\pi}{\delta}$	δf_o	$\frac{1}{\delta f_o}$	$\frac{6.9}{\delta f_o}$	$8.69f_o\delta$	δ

Table 1. Interrelations between measures of damping

critically damped. A critically damped system will as free vibrations show an exponentially decaying vibration without free oscillations.

In this article measurement of the *fraction of critical damping* is used exclusively for the comparison of the different methods.

Measurement Conditions and Equipment Used

The damping measurements were performed on a freely suspended and thus extremely lightly damped aluminium plate with the dimensions of 30cm x 25cm x 2cm. The structure was for some measurements excited by an impact hammer Brüel&Kjær Type 8202 (see Fig. 1) with a built-in Brüel&Kjær Force Transducer Type 8200. The steel tip was used to ensure proper excitation in the frequency range of interest which was from 500 Hz to 3kHz, a range that includes the first five modal frequencies.

In other situations the structure was excited via a nylon stinger by a small Brüel&Kjær Vibration Exciter Type 4810 (see Fig.1) using either a Random or a Pseudo Random signal. The input force was also in these cases measured using a Brüel&Kjær Force Transducer Type 8200.

The output vibration signal was measured using a small lightweight (~2.4g) Brüel&Kjær Accelerometer Type 4375. The force and vibration signals were analyzed using either the Brüel&Kjær Multichannel Analysis System Type 3550 (DFT/FFT) or the Brüel&Kjær Dual Channel Real-time Frequency Analyzer Type 2133 (DF). All results were plotted on a Brüel&Kjær Graphics Plotter Type 2319. Post-processing of data was in some cases carried out using the SMS modal software STAS SE (Brüel&Kjær Type number WT9100), the Brüel&Kjær 3D-plot of spectra software Type WT9321 and the Brüel&Kjær Non-stationary Signal Analysis Software Type WT9362.

Using the digital filter analyzer the damping was estimated by the Schroeder method, also called "Integrated Impulse Response Method" (Ref.[9]).

Experimental Results using Digital Filter Analysis

The damping is here estimated from the decay of the free vibration response due to an impact excitation. The plate structure was excited by an impact hammer in a comer point ensuring excitation of the first five modes of interest. The acceleration was measured in another comer ensuring that the response from the modes of interest were all included in the measured

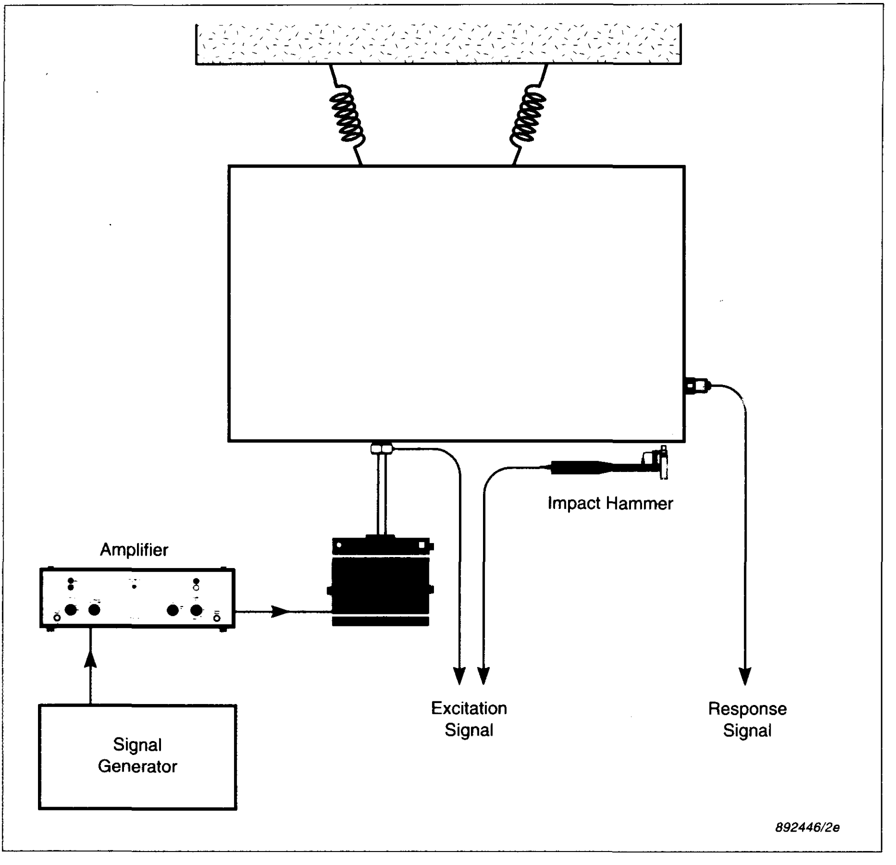

Fig. 1. Measurement configuration/setup shown without the frequency analyzers

response signal. 1/12 octave bandwidth was selected in order to have the resonance frequencies separated in different analysis bands. This makes estimation of the damping for each mode of vibration possible. Exponential averaging, T_A of 1/32 sec was used which means that a reverberation time $T_{60} > 14 \cdot T_A$ = 14/32 sec = 0.44 sec could be estimated with sufficient accuracy (see Ref. [3]). The Brüel&Kjær Real-time Frequency Analyzer Type 2133 can store spectra at specified time intervals in a multi-spectrum. In this experiment 200 spectra of the response signal were stored with an interval of 25 msec between spectra. Fig. 2 shows the measurement setup in the analyzer and the slice of the multispectrum at 866 Hz i.e. the 1/12 octave band at 866 Hz, containing the 1st resonance, as a function of time. The amplitude is presented on a logarithmic dB scale which means that the exponential decay

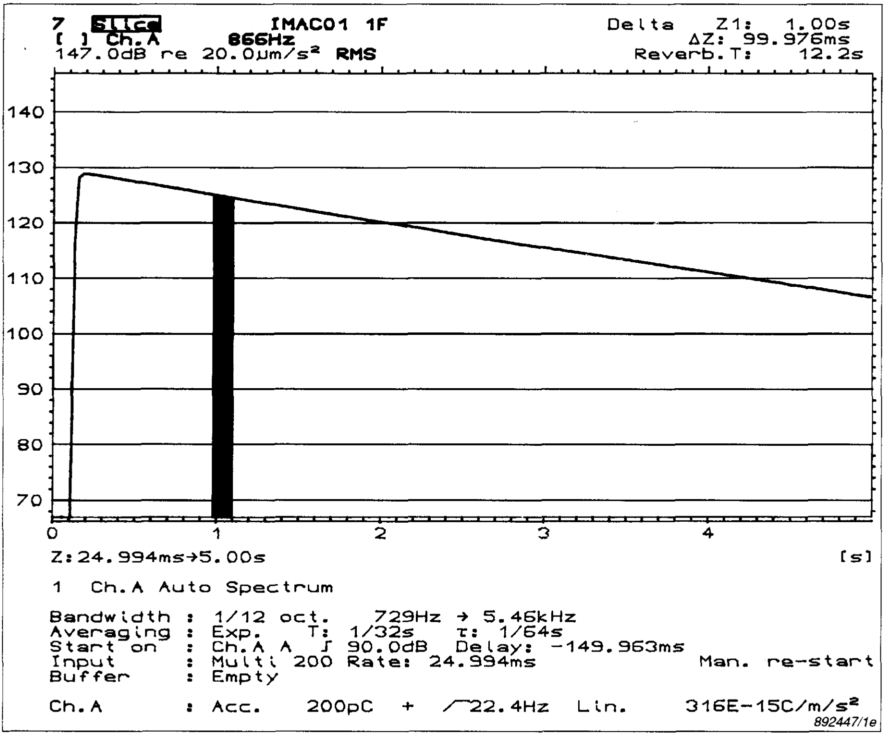

Fig. 2. Measurement setup for the analysis and decay of the 1st resonance in the 1/12 octave band at 866 Hz

$$A(t) = A_o e^{-\sigma t} \quad (1)$$

will appear as

$$10\log\,[A\,(t)/A_{ref}]^2 = 10\log\,[A_o/A_{ref}]^2 - \sigma \cdot t \cdot 10\log e^2$$

$$= C_o - 8.69 \cdot t \cdot \sigma$$

$$= C_o - 8.69 \cdot t/\tau \qquad (2)$$

i.e. as a straight line with a slope of -8.69dB · σ = 8.69dB/T, where σ is the decay constant and τ the time constant of the resonance. C_o is the maximum level of the response and depends upon the amplitude and the spectral shape of the impact as well as the position of the excitation and response measurement. The reverberation time, $T_{60} = 6.9\tau$, calculated from the slope of the slice in the highlighted part of the graph, defined by a delta cursor, is given in the upper right comer of the plot.

Fig. 3 shows a 3D plot of vibration decays in the 1/12 octave bands. The five modes of interest are clearly seen in the plot in the 866 Hz, 1220 Hz, 1730 Hz, 2050 Hz and 2300 Hz 1/12 octave bands. Due to the non-ideal amplitude characteristic of the filters (6 pole filters) energy has leaked into the neighbouring frequency bands. The initial broadband excitation is seen as well.

The slices of the 2nd and the 3rd resonance in the 1220Hz and 1730Hz band are shown in Fig. 4. The decays have here been backwards integrated, see Ref. [9], in order to obtain smooth decays and well defined initial levels for automatic reverberation time calculations. The reverberation time for all the bands were estimated from the backwards integrated decays in an evaluation range from 5dB to 25 dB below the initial level, except for the 866 Hz band where the evaluation range was set between 5dB and 15 dB below the initial level. This was due to the long reverberation time for the 1st resonance. The reverberation time spectrum is given in Fig. 5 a. and in tabular form in the left column of Fig. 6.

The reverberation time is then converted (see Table 1) to the fraction of critical damping ζ by

$$\zeta = 1.1/f_o \cdot T_{60} \qquad (3)$$

where f_o is undamped natural frequency of the resonance. For the calculations the centre frequency of the 1/12 octave bands are used for f_o, which

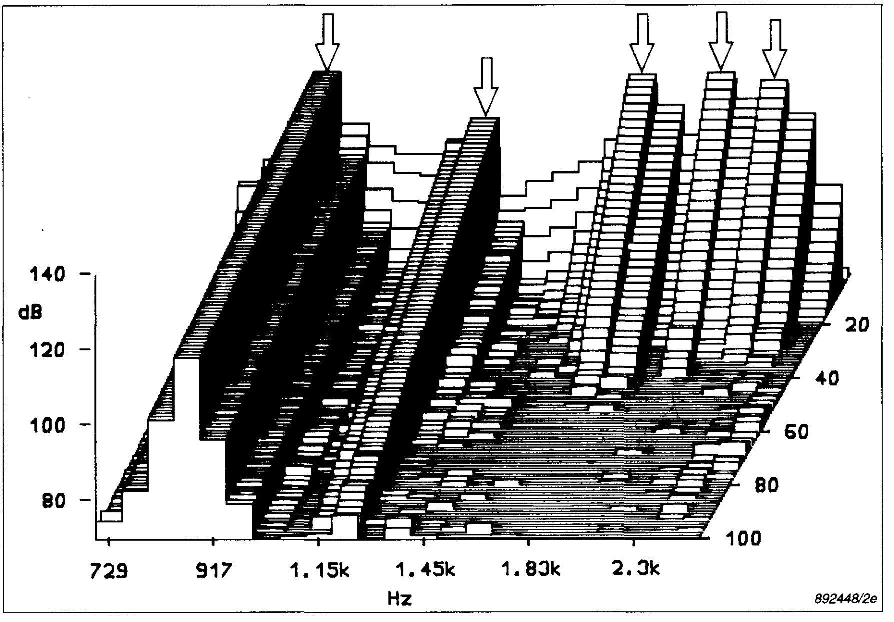

Fig. 3. 3D plot of the first 100 spectra of the multispectrum showing the vibration decay in 1/12 octave bands. The 5 bands containing the resonances are indicated by arrows

imposes an uncertainty of maximum 3% on the results. The spectrum of the percentage of critical damping ($\zeta\% = 100 \cdot \zeta$) called C_r. Damping is shown in Fig.5b and in tabular form in the right column of Fig. 6. The values for the percentage of critical damping are inserted in Table 2.

A reverberation time and thus a damping value has been calculated in some of the bands not containing a resonance. This is due to the leakage effect caused by the non-ideal filtershape in the analysis as mentioned earlier. For those bands where a T_{60}, and thus ζ, could not be calculated, a warning line is indicated below the frequency axis in the spectrum and an empty space is left in the table.

One advantage of this method is that it is extremely fast. After one hammer impact the damping values are automatically calculated in the analyzer without any operator interference. Also this method has practically no limitations in dealing with very lightly damped systems.

For single resonance damping measurements the basic requirement is however that the resonances are separated in different bands. Otherwise the cal-

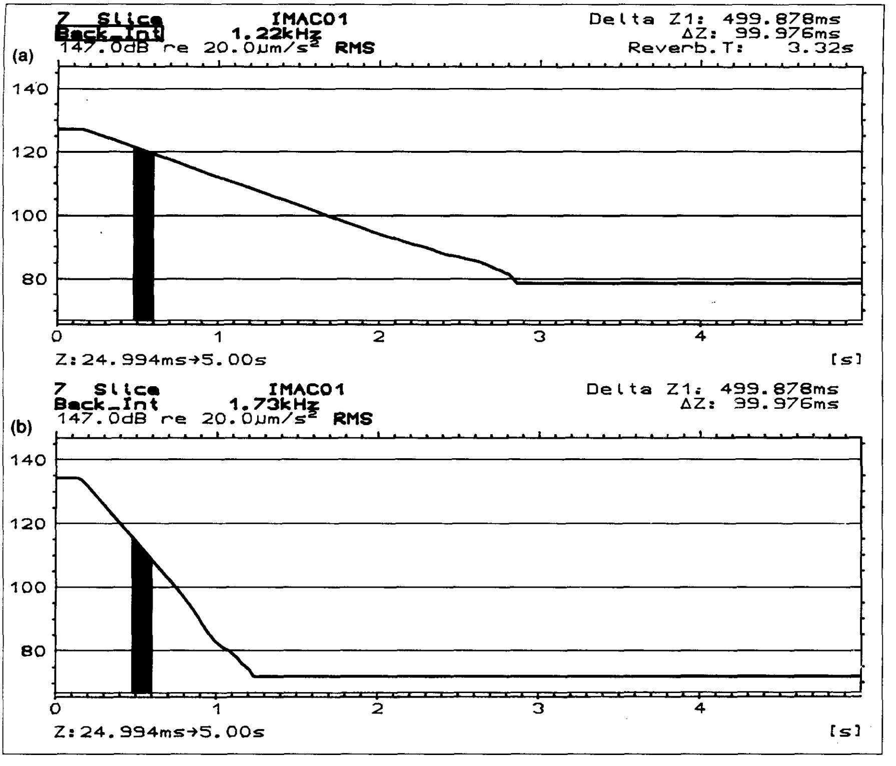

Fig. 4. Decay curves for the 2nd and the 3rd resonance in the 1/12 octave bands at 1220 Hz and 1730Hz. The decays have been backwards integrated in order to give smooth decays and well defined initial levels (used for reverberation time calculations)

culated damping values will depend upon how the test is performed (excitation point and response point) and how the reverberation time is calculated. In situations with high modal density i.e. many mode within each band this method will give an average damping value of the modes. This will normally require averaging of the decay curves over several measurement and excitation points. This multipoint technique is extremely useful and very often required in acoustical applications.

The upper limit of damping values which can be handled by this method will depend upon the bandwidth and the integration time in the detector. This is discussed in the following section.

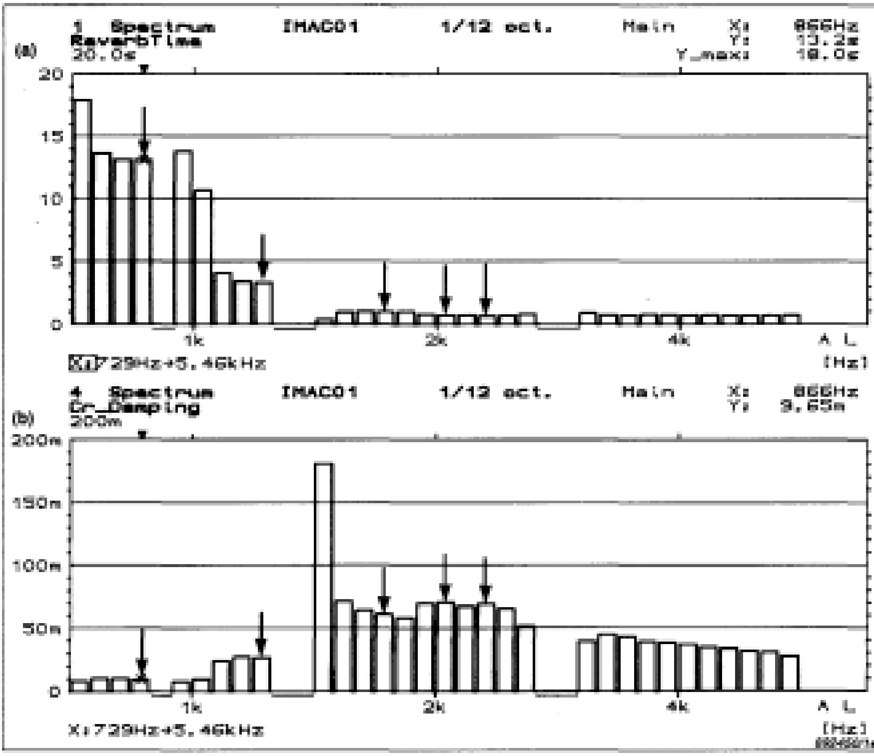

Fig. 5. Spectrum of the a) calculated reverberation time and b) calculated fraction of critical damping (in percent ζ%). The 5 bands containing the resonances are indicated by arrows

Time Reversed Decay Measurements

Using "classical" analysis techniques, i.e. filtering in 1/3 or 1/1 octave bands, limitation exists due to "ringing" in bandpass filters and smoothing caused by the detector.

According to Ref.[3] reliable decay curves are obtained only if the fraction of critical damping is less than 0.017 (1.7%) for 1/3 octave analysis. For 1/1 octave and 1/12 octave analysis the limits are 3 times higher and 4 times lower respectively.

However, in Ref. [4] it has been demonstrated that reversing the time signal to the filters leads to much less distortion on the decay curve and reliable

1 Spectrum IMAC01 1/12 oct. Main X: 866Hz
ReverbTime Y: 13.2s
20.0s
X:729Hz→5.46kHz

Freq. Hz	ReverbTime s	Cr_Damping
866	13.2	9.65m
917		
972	13.8	8.20m
1.03k	10.7	9.97m
1.09k	4.13	24.5m
1.15k	3.47	27.5m
1.22k	3.36	26.7m
1.30k		
1.37k		
1.45k	419m	181m
1.54k	992m	72.0m
1.63k	1.05	64.3m
1.73k	888m	71.7m
1.83k	884m	68.0m
1.94k	888m	63.9m
2.05k	851m	62.9m
2.18k	750m	67.4m
2.30k	686m	69.6m

4 Spectrum IMAC01 1/12 oct.
Cr_Damping Y: 9.65m
200m
X:729Hz→5.46kHz 892451/1e

Fig. 6. Table of the reverberation time spectrum and the fraction of critical damping (in percent ζ %) spectrum. The 5 bands containing the resonances are indicated by arrows

damping measurements on four times more damped systems can be performed. Thus for 1/3 octave analysis the fraction of critical damping should be less than 0.07 (7%).

When measuring on highly damped structures (short decay curves) it is important to choose the averaging time of the detector short enough to avoid influence on the decay curve. On the other hand we should also choose an averaging time as long as possible in order to minimize statistical errors. Using a device with exponential averaging (time constant, τ_d corresponding to an averaging time, $T_{AV} = 2\tau_d$) the averaging time should obey

$$\tau_s > 2\tau_d \tag{4}$$

where τ_s is the time constant of the system under test. The factor of 2 is due to the fact that the averaging is performed on the squared output of the filters. Thus τ_s is the time taken for the signal amplitude to decay 8.68 dB while τ_d is the time it takes for the averaging device to decay 4.34 dB.

In Ref. [3] the factor for the inequality (4) is chosen as four

$$\tau_s > 4\tau_d, \tag{5}$$

to be on the safe side.

Fraction of critical damping					
	ζ_1% (860 Hz)	ζ_2% (1198 Hz)	ζ_3% (1756Hz)	ζ_4% (2091 Hz)	ζ_5% (2341 Hz)
Free decay DF 1/12 octave	0.0097	0.0267	0.0717	0.0629	0.0696
Free decay FFT Δf = 8Hz	0.0103	0.0261	0.0738	0.0625	0.0696
Curvefit Baseband Impact*	0.273	0.215	0.193	0.178	0.161
Curvfit Baseband Impact Corrected	0.0093	0.0250	0.0643	0.0688	0.0640
Curvefit Baseband Random*	0.029	0.108	0.177	0.130	0.144
Curvefit Zoom Random	0.011	0.029	0.066	0.071	0.063
IRF decay Baseband Pseudo Random	0.0134	0.0286	0.0633	0.0662	0.0633
Curvefit Baseband Pseudo Random	0.013	0.029	0.063	0.066	0.063
IRF decay Zoom Pseudo Random	0.0121	0.0275	0.0703	0.0672	0.0657

*Table 2. Damping values, fraction of critical damping in percent ζ %, from the different test methods. Those values in the rows indicated with an * are heavily biased as expected*

However since the response of the detector is much faster when the signal increases instead of decreasing it will be of great advantage to use time reversed analysis. According to Ref.[4] the requirements (5) can be replaced by

$$2\tau_s > \tau_d \tag{6}$$

Thus it is possible to measure eight times higher damping factors without the need for decreasing the averaging time by a factor of eight.

Experimental Results Using FFT Techniques

The damping was here measured using the following methods:

a) Free vibration decay
b) Curve fit of frequency response functions measured using impact excitation
c) as b) but using random excitation with a shaker
d) Decay of impulse response function calculated from weighted frequency response function using pseudo random excitation with a shaker. These results were compared with results of curve fit of the frequency response function.

In all the measurements the Brüel&Kjær Multichannel Analysis System Type 3550 was used.

a) Free Vibration Decay

The free vibration decay technique used here was similar to the technique just described using digital filtering.

A frequency resolution of ΔF = 8Hz was selected on the analyzer which means that the time record $T = 1/\Delta F$ =125 ms was sufficiently short to follow the decay of the signal. Averaging was set to exponential of 1 which means that the autospectrum is the magnitude of the instantaneous spectrum (i.e. no averaging). The FFT was performed with Hanning weighting on the time signal. 400 frequency lines from 0 Hz to $400 \cdot \Delta F$ = 3200 Hz were transferred to the multibuffer every 25ms. A 3D plot of the autospectra in the multibuffer is shown in Fig.7. The decay of the 5 resonances is clearly seen. The initial broadband response due to the impact is also seen.

The resonances appeared in the frequency lines at 864 Hz, 1220 Hz, 1760hz, 2096 Hz and 2352 Hz. The slices along these frequencies are shown in Fig. 8 and from the slope of these the decay rate, and thus the fraction of critical damping can be determined via a User-definable Auxiliary Information (see Table 1). The results are inserted in Table 2.

As expected the results agree very well with the results from the test using DF. As for the free decay method using DF there is practically no lower limit for the damping values which this method can handle. The requirement is that only one resonance resides in each analysis bandwidth (i.e. only one resonance per three analysis lines when Hanning weighting is used). The upper limit for the damping values to be estimated by this method comes from the storage rate of spectra (typically in the order of 20 to 100 spectra per second) which depends on the transform size and the speed of FFT calculations.

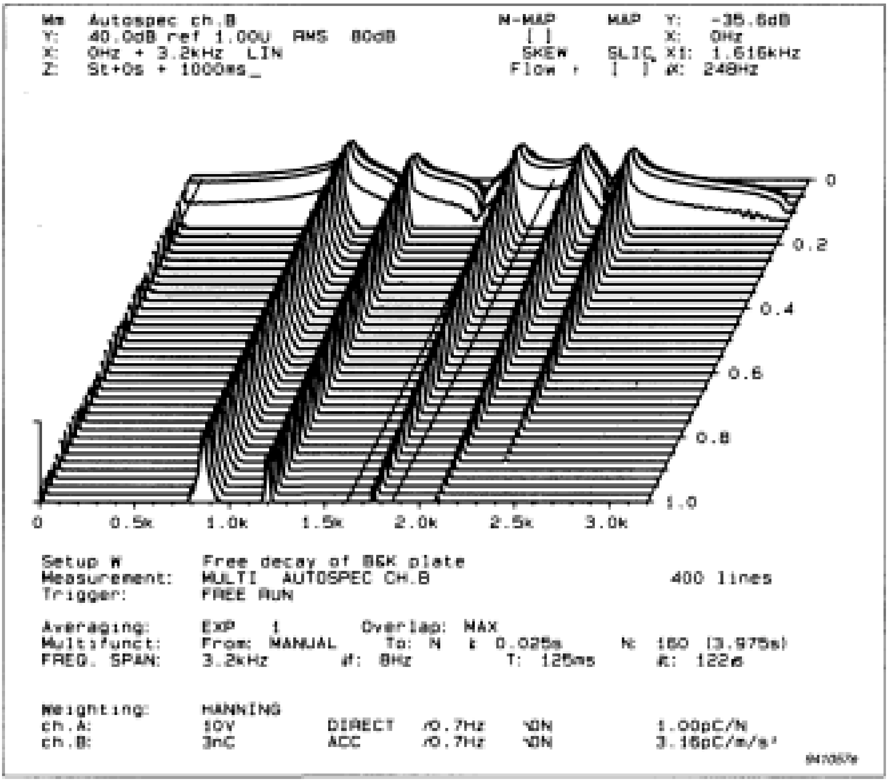

Fig. 7. 3D map of FFT spectra of free vibration decay. Interval between spectra is 25 msec and 400 frequency lines cover the span from 0 Hz to 3200Hz with a resolution of Δf= 8Hz. Only the first second of the 4 sec recording is shown

If the decay is too fast (i.e. the damping is too high) another possibility is to record the response signal in a time buffer sufficiently long to contain the whole signal (or most of it). For the Multichannel Analysis System Type 3550 a (64 K sample buffer) Time Capture and a (700 K sample to disk) Time History modes are available. The advantages of recording into a buffer is that any (high) overlap between the spectra in the 3-D plot is obtainable, thus giving us a good time resolution. See Fig. 9.

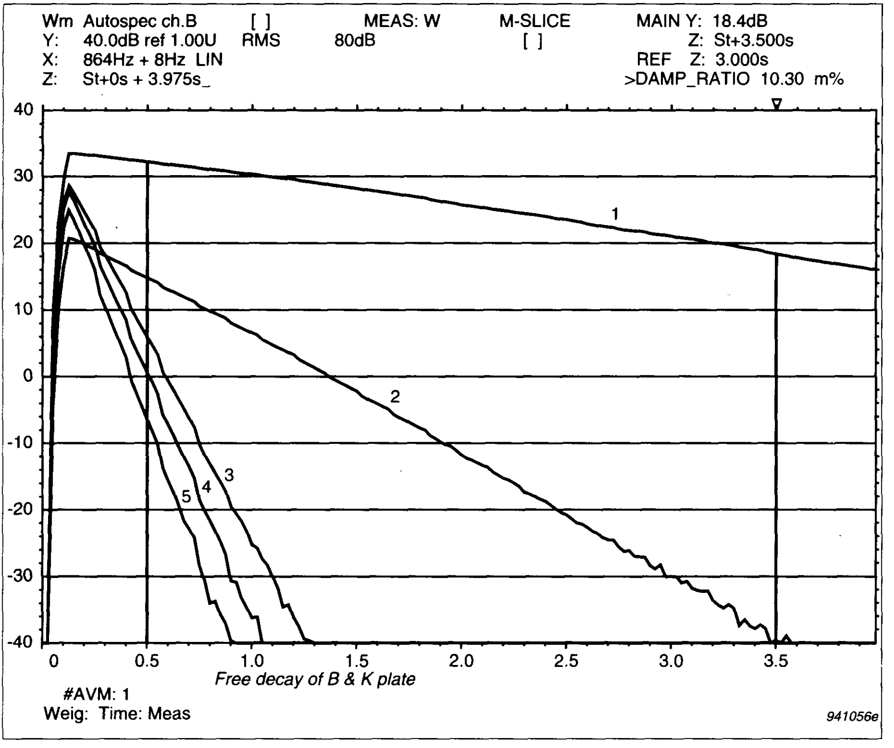

Fig. 8. Plot of the slices at the resonances giving the decay of vibrations. The frequency lines containing the resonance are 1) 864Hz, 2) 1200Hz, 3) 1756Hz, 4) 2096Hz, and 5) 2340Hz

b) Curve Fit of FRFs measured using Impact Excitation

Instead of only measuring the acceleration response the impact force is also measured here and from the two signals the frequency response function (acceleration/force i.e. accelerance) is estimated using dual channel FFT calculation. Fig. 10 shows measurement setup and an estimated accelerance function. A frequency range of 3.2kHz with a line spacing of ΔF = 4 Hz was selected giving a record length of T= 250msec. Since the response signal is much longer than 250msec an exponential weighting function with a time constant of 50msec (given as length in the setup) is applied to the response signal in channel B. The force impulse is measured in channel A with a tran-

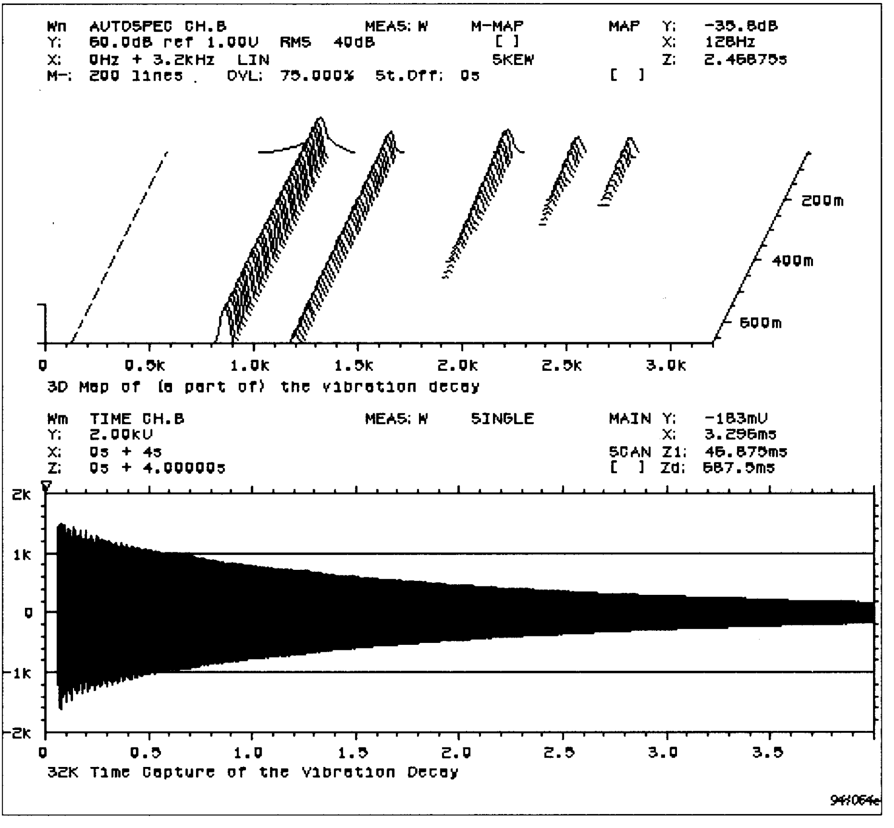

Fig. 9. Time Capture Recording of 32K samples corresponding to 4 sec recording using 3,2 kHz range. The scan cursor has been applied to produce a 200 line 3D map with 75% overlap of the data. A map of the first 625ms is shown

sient weighting function. The response signal is in Fig. 11 shown with and without multiplication of the exponential weighting. Notice that the signal is attenuated more than a factor of 100 at the end of the record with the exponential weighting ensuring a well denned influence of leakage in the analysis (to be corrected for later).

The frequency response function is transferred to the modal analysis software (SMS STAS SE) where curve fitting of the individual resonances is performed. SDOF polynomial curvefitting is used and the resulting damping values (percentage of critical damping) are given in Table 2.

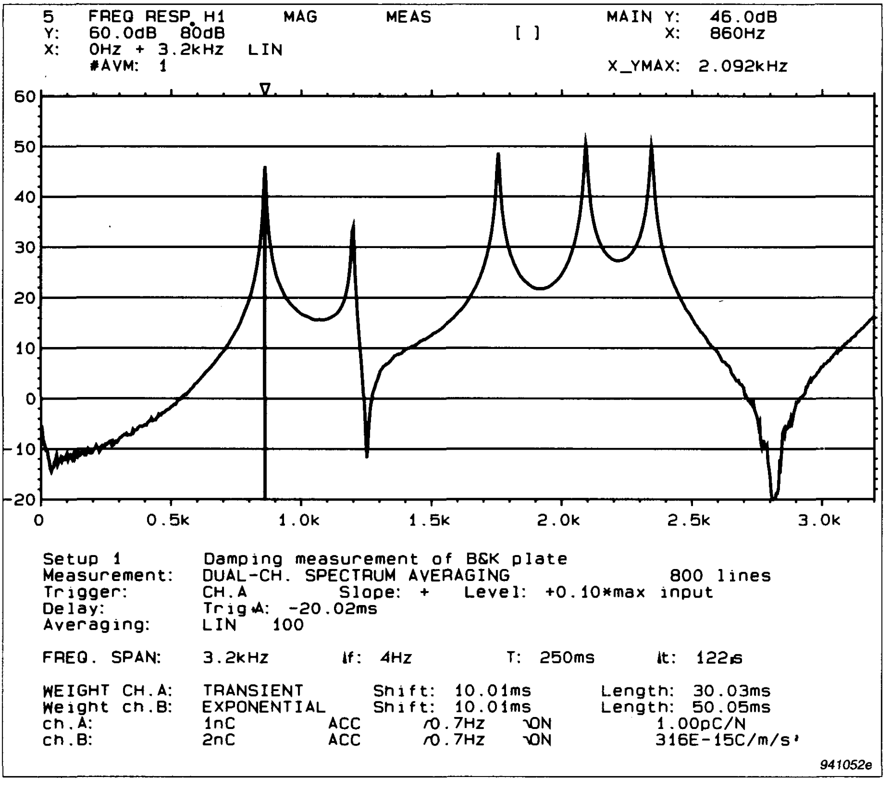

Fig. 10. Measurement setup for frequency response function measurement using impact hammer excitation and an estimated frequency response function (accelerance)

From the modal parameters, frequency, damping and residue, obtained from the curve fitting for the five modes, the frequency response function is synthesized and shown on top of the measured function in Fig. 12. Excellent agreement is observed indicating proper curve fitting. Such synthesis and comparison is also possible inside Multichannel Analysis System Type 3550 using User Definable Functions and superimposed format.

The estimated damping values are too high due to the exponential weighting. The influence of the weighting function is however well defined and can be corrected for as follows (see Ref. [10]).

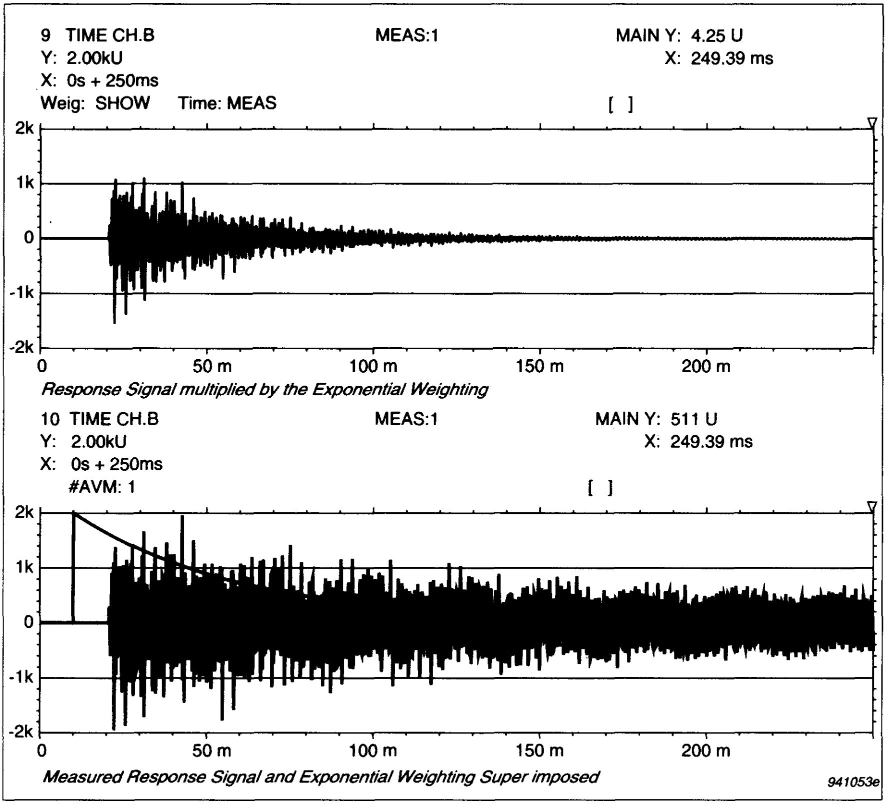

Fig. 11. Response signal (acceleration) with (a) and without (b) multiplication of the exponential weighting function

$$\begin{aligned}\zeta_{corr} &= \zeta - \zeta_w \\ &= \zeta - \frac{1}{2\pi f_0 \tau_w}\end{aligned} \tag{7}$$

where ζ is the estimated damping, ζ_w, is the damping from the exponential weighting, τ_w is the time constant (length) of the exponential weighting and f_0 is the natural frequency of the mode. Such correction is provided in the modal software and the results are given in Table 2. Excellent agreement with the previous results are obtained.

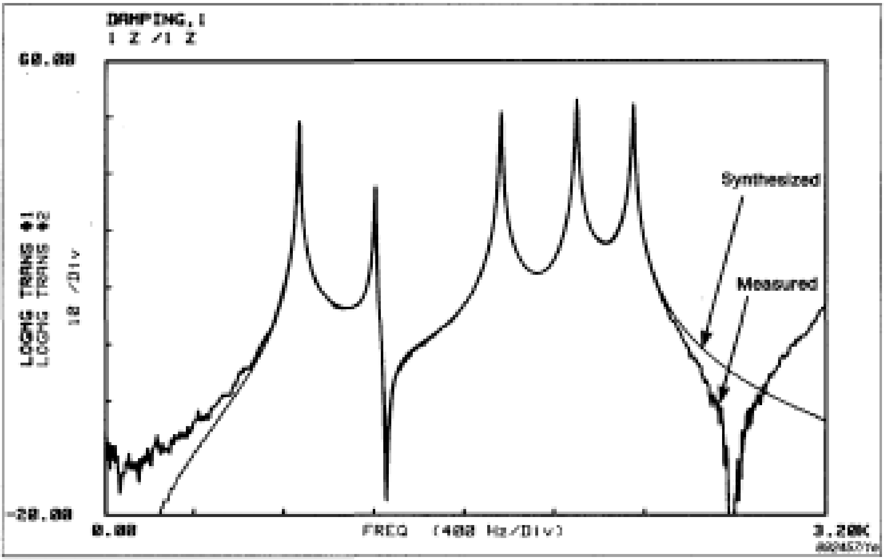

Fig. 12. Measured and synthesized frequency response function. The five modes were curve fitted using SDOF polynomial curve fitter

The advantage of this method, compared to the free decay methods (DF or FFT), is that very damped systems (vibration decay within the record length T) and systems with high coupling between the modes can be analysed. In situations with heavy coupling between the modes a MDOF curve fitter would have to be applied.

c) Curve Fit of FRFs measured using Random Excitation

The frequency response function (accelerance) is here estimated using a shaker and a random force signal as excitation. First a baseband measurement with a frequency span of 3.2kHz and resolution of ΔF = 4 Hz was used as for the impact hammer test b). The measurement setup and an estimated frequency response function is shown in Fig. 13. The levels of the resonances and the location of the anti-resonances is different from the impact test (Fig. 10) because the excitation is in a different point. This will however only affect the residues (which are local parameters) and not the frequency and damping values (which are global parameters for the structure).

Using only 4 Hz resolution the resonance peaks are however heavily affected by leakage as indicated by the low coherence at the resonance frequencies

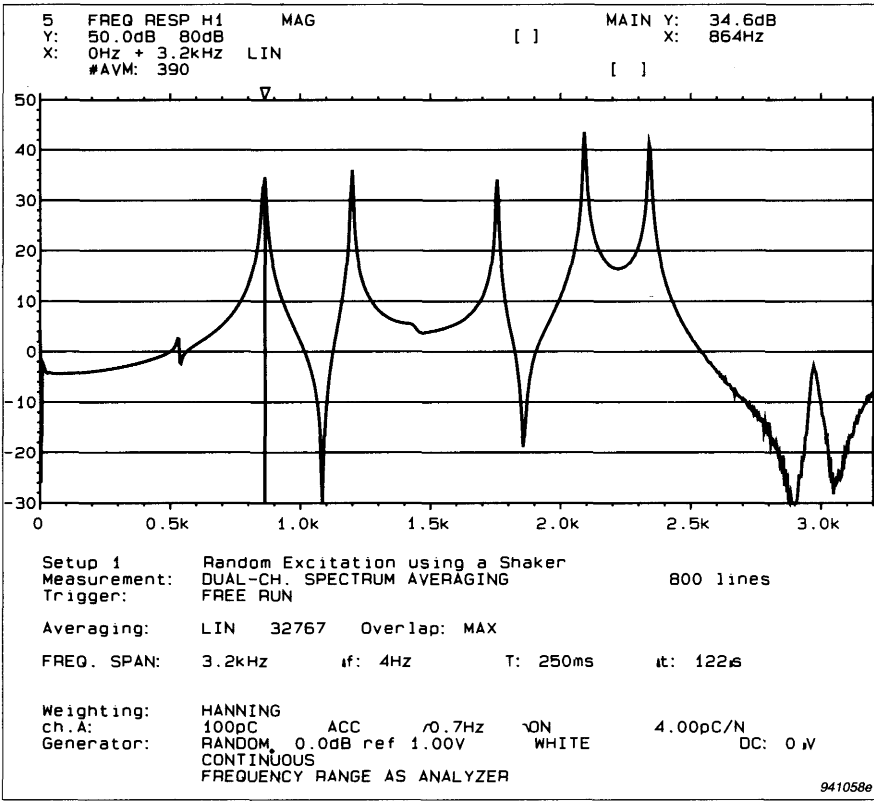

Fig. 13. Measurement setup and estimated frequency response function using random excitation with a shaker

(Ref. [10]) as shown in Fig. 14. The too low values of the frequency response function at the resonances is also called resolution bias due to the insufficient resolution in analysis.

Again the frequency response function was transferred to the modal software and the individual resonances were curve fitted using SDOF polynomial curve fitter.

The resulting damping values are found in Table 2. As expected the damping values are severely overestimated due to the leakage in the analysis. In order to avoid the influence of leakage (or resolution bias errors) 5 zoom measure-

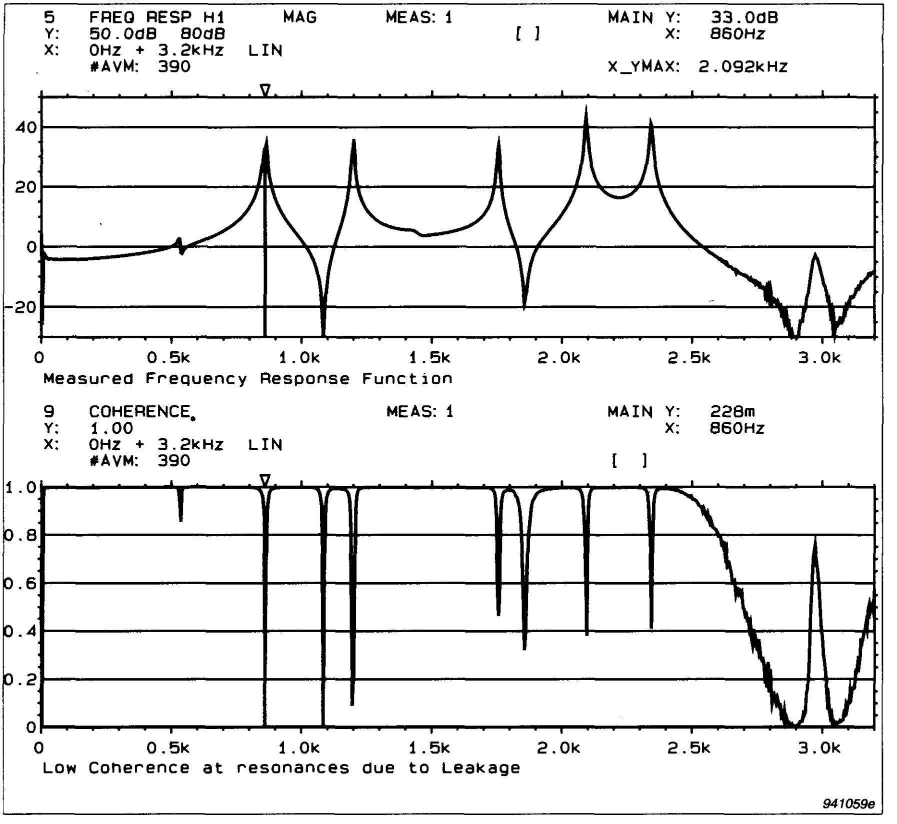

Fig. 14. Frequency response function and coherence in the baseband measurement using random force excitation. Notice the low coherence at the resonances due to leakage (resolution bias error)

ments were performed around each resonance with sufficient resolution so effect of leakage were eliminated.

The following resolutions were required:

ΔF = 7.8125 mHz for mode 1 at 860 Hz
ΔF = 62.5 mHz for mode 2 at 1198 Hz
ΔF = 125 mHz for mode 3 at 1756 Hz
ΔF = 125 mHz for mode 4 at 2091 Hz
ΔF = 125 mHz for mode 5 at 2341 Hz

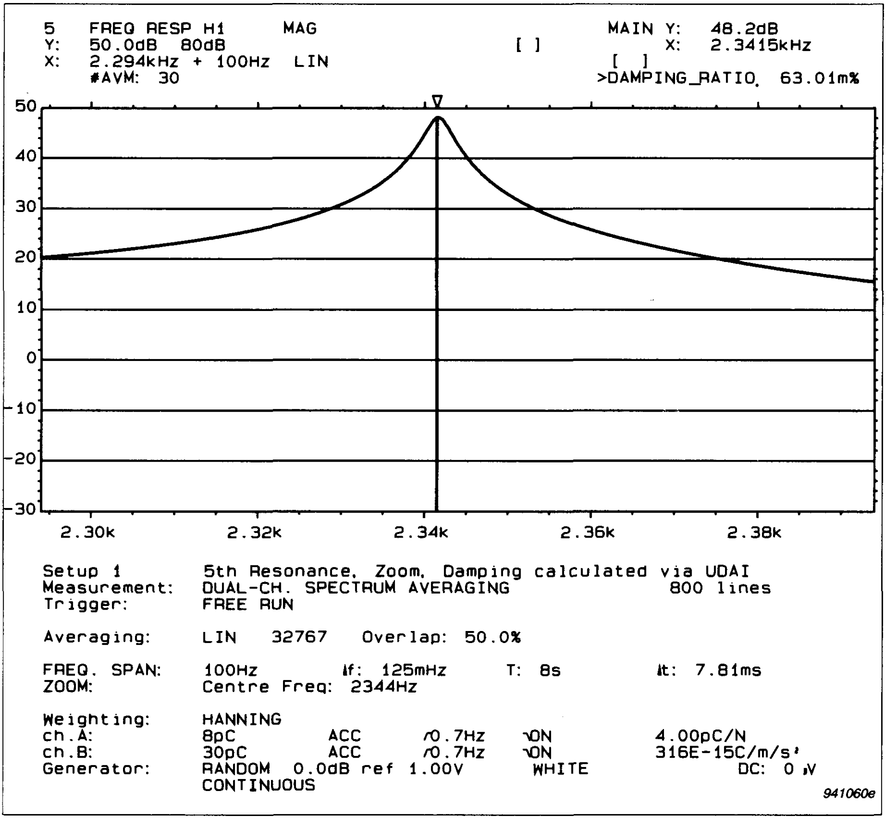

Fig. 15. Zoom measurement around the 5th resonance, Damping Calculated via a User Definable Auxiliary Information

This resolution ensured more than 10 frequency lines in the analysis within the 3 dB bandwidth Δf of the resonances. The force spectrum was very low at the resonance frequencies and thus contaminated with noise at these frequencies. $H_2(f)$ was used as the estimate of the frequency response function since $H_2(f)$ is immune against uncorrelated noise at the input (Ref. [10]).

For each Zoomed Frequency Response Function, damping could be calculated directly inside the analyzer using a User Definable Auxiliary Information see Fig.15. The results are given in Table 2. Except for the first two modes these damping values agree very well with those obtained from the decay methods and the corrected values from method b). The higher value of the damping for mode 1 and 2 is probably caused by the influence of the force transducer attached to the structure at the excitation point.

The disadvantage of the zoom technique is the extremely long analysis time required, specially for the first mode. The record length was here $T = 1/\Delta F = 1/7.8125$ mHz = 128 sec, which means that e.g. 20 statistical independent averages performed with 50% overlap took (128+19 · 128/2)sec = 1344sec = 22min 24 sec.Ref.[12].

d) Decay of Impulse Response Function Calculated from Weighted Frequency Response Function

The frequency response function (accelerance) is estimated using shaker excitation as in c) here however, with a pseudo random force signal. The pseudo random signal is a periodic signal with a period length T equal to the record length T in the analyzer. The sinusoidal components in the spectrum thus coincides with the analysis lines in the analyzer and leakage is avoided using rectangular weighting (Ref.[101). The calculated lines in the frequency response function are thus samples of the "true" frequency response function and can be used for calculation of unbiased (with respect to damping) impulse response function or leakage-free curve fitting.

A baseband measurement with a frequency span of 3.2kHz (as previously) is performed. The measurement setup and an estimated frequency response function is shown in Fig. 16. A frequency weighting function consisting of a short rectangular weighting with 50% cosine taper were then used to isolate the different resonances in the frequency response function. Fig. 17 and 18 shows the weighted frequency response function and the corresponding impulse response function (magnitude) for mode 1 and 5 respectively. The decay appears on a logarithmic amplitude axis as a straight line. The damping is now extracted from the measured slope of the decay exactly as was done in the free decay method. A User Definable Auxiliary Information is used for the damping calculation. The resonance frequency is defined as a User Definable Variable. The reference cursor was used to define the two cursor points as seen in Fig. 17 and 18. The resulting damping values calculated by the User Definable Auxiliary Information are given in Table 2 and excellent agreement with the values from the zoom measurements in the random test c) is obtained except for the 1st mode where $\zeta_1 = 0.0134\%$ instead of $\zeta_1 = 0.011\%$. This could be caused by problems with uncorrelated noise in the input (force) at the resonances. The impulse response function was calculated from $H_1(f)$ which, as opposed to the $H_1(f)$ estimator, is biased (too low amplitude values) in case of

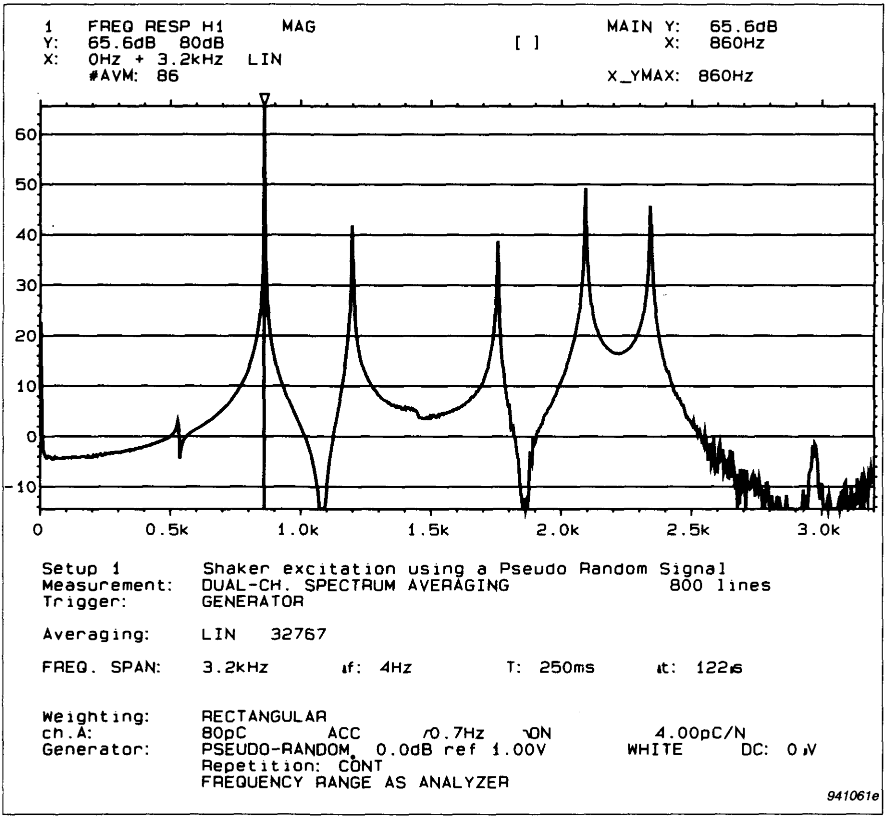

Fig. 16. Measurement setup and estimated frequency response function using pseudo random excitation with a shaker

noise at the input. The estimated damping values will thus be biased as well (too high).

The baseband frequency response function ($H_1(f)$) was also transferred to the modal software and SDOF polynominal curve fitting was performed on each resonance. The damping results are given in Table 2 and they are seen to be identical to the values estimated from the impulse responses.

Finally 100 Hz wide zoom measurements with ΔF = 125 mHz were performed around each resonance in order to investigate whether there was any influence of input noise as mentioned earlier. With ΔF = 125 mHz the signal/

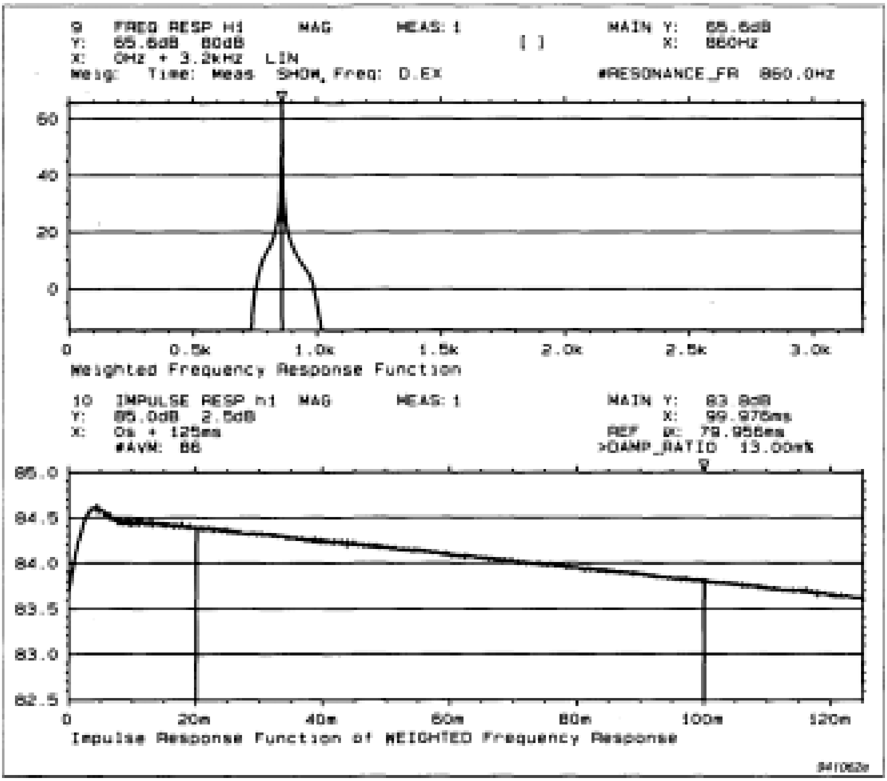

Fig. 17. Weighted frequency response function isolating the 1st resonance and corresponding impulse response function (magnitude). The weighting function is a transient window 40 frequency lines wide with 20 lines cosines taper on each side (50% cosine taper)

noise ratio is improved by a factor of 32 (15dB). The record length T is here 8 sec. The damping values calculated from the impulse responses of the zoom measurements are given in Table 2. For the 1st mode the damping is now estimated to be ζ_1= 0.0121% which is closer to the value from the random test with zoom. The damping values of the 3rd 4th and 5th mode gave, however, slightly higher values compared to the baseband test. The estimated damping values thus seems to be more influenced by small random errors than by systematic errors from the noise problem. This method, using pseudo random excitation, is thus much faster than the one using random excitation, since a

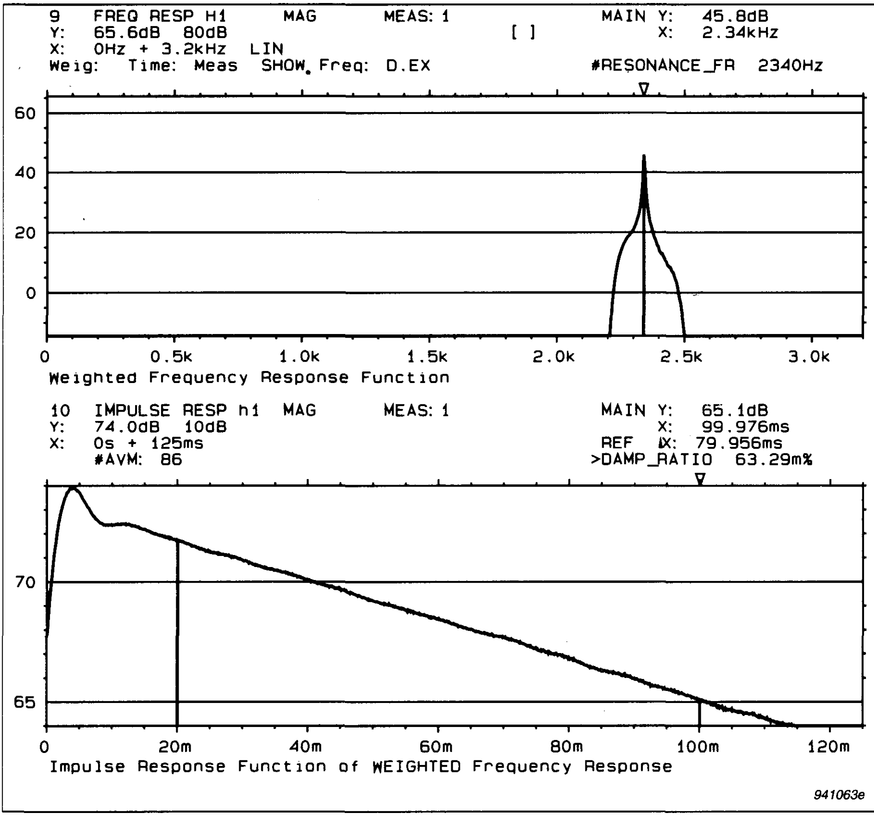

Fig. 18. Weighted frequency response function isolating the 5th resonance and the corresponding impulse response function (magnitude). The weighting function is a transient window 40 frequency lines wide with 20 lines of cosine taper on each side (50% cosine taper)

(baseband) measurement where $\Delta F \approx 50 \cdot \Delta f$ gives damping results within the overall accuracy determined by the setup. Ref. [16].

As for the decay methods, damping of single modes can only be determined if the modes are well separated in the spectrum (say by 10 analysis lines in this case). Otherwise an average damping of the modes in the bandwidth (determined by the frequency weighting function) is obtained and averaging over several excitation and response points would have to be performed in order to get consistent results.

Experimental Results Using Time-frequency Analysis Techniques

The Brüel&Kjær Non-stationary Signal Analysis Software, WT9362 offers three advanced Time-frequency analysis techniques, namely the Short-time Fourier Transform (STFT), the Wavelet Transform (WT) and the Wigner-Ville Distribution (WVD). Refs. [13,14,15].

Since signals from vibration decay measurements are highly non-stationary, these techniques are well suited for damping calculations using the free decay method.

STFT provides constant absolute bandwidth analysis, which is often preferred with vibration signals in order to identify harmonic components. STFT offers a constant resolution in time as well as in frequency domain irrespective of the actual frequency. The STFT is denned as the Fourier Transform of a Gaussian windowed time signal for various positions, b, of the window. This can be stated in terms of inner products between the signal and the window:

$$\mathrm{Sb} = \int s\,(t)\, g^*\,(t-b)\, e^{-j2\pi f\,(t-b)}\mathrm{dt}$$

$$= \langle s,\, g_{b,f}\rangle$$

$$\text{with } g_{b,f}(t) = g\,(t-b)\, e^{j2\pi f\,(t-b)} \tag{8}$$

where s is the signal, g is the window, b is the time parameter and fis the frequency parameter. See Fig. 19.

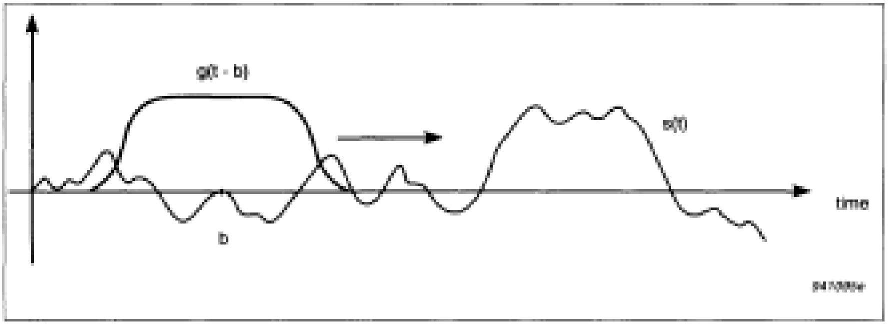

Fig. 19. The Short-time Fourier Transform (STFT). The Window, g(t - b) extracts spectral information from the signal around time b by means of the Fourier Transform

The Wavelet Transform (WT) is especially relevant for acoustic applications since it provides constant percentage bandwidth analysis (e.g. 1/3 octaves). Thus WT offers excellent frequency resolution at low frequencies and excellent time resolution at high frequencies. The WT is denned from a basic wavelet, ψ, which is an analyzing function located both in time and frequency. From the basic wavelet a set of analyzing functions is found by means of scalings (parameter a) and translations (parameter b):

$$
\begin{aligned}
S(b, a) &= a^{-1/2} \int s(t)\, \psi^* \left(\frac{t-b}{a}\right) dt \\
&= \langle s, \psi_{b,a} \rangle \\
\text{with} \quad \psi_{b,a}(t) &= a^{-1/2}\, \psi \left(\frac{t-b}{a}\right)
\end{aligned}
\tag{9}
$$

where s is the signal, ψ is the wavelet, b is the time parameter and a is the scale parameter. See Fig. 20.

The product between time (RMS duration) and frequency (RMS bandwidth) resolution cannot be smaller than 1/4 π for these two techniques, according to the Heisenbergs Uncertainty Principle.

The Wigner-Ville Distribution (WVD) is not limited by the uncertainty relationship, due to the fact that it is a more general transform, not using an analyzing function. Unfortunately this transform leads to the emergence of negative energy levels and cross terms, which are irrelevant from a physical point of view. Therefore the analysis results obtained with WVD can some-

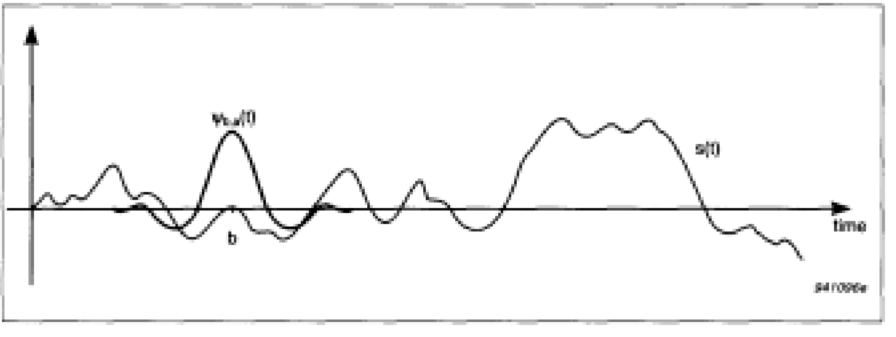

Fig. 20. The Wavelet Transform (WT). The Wavelet, ψ , extracts time scaled information from the signal around the time, b by means of inner products between the signal and scaled (parameter a) versions of the wavelet

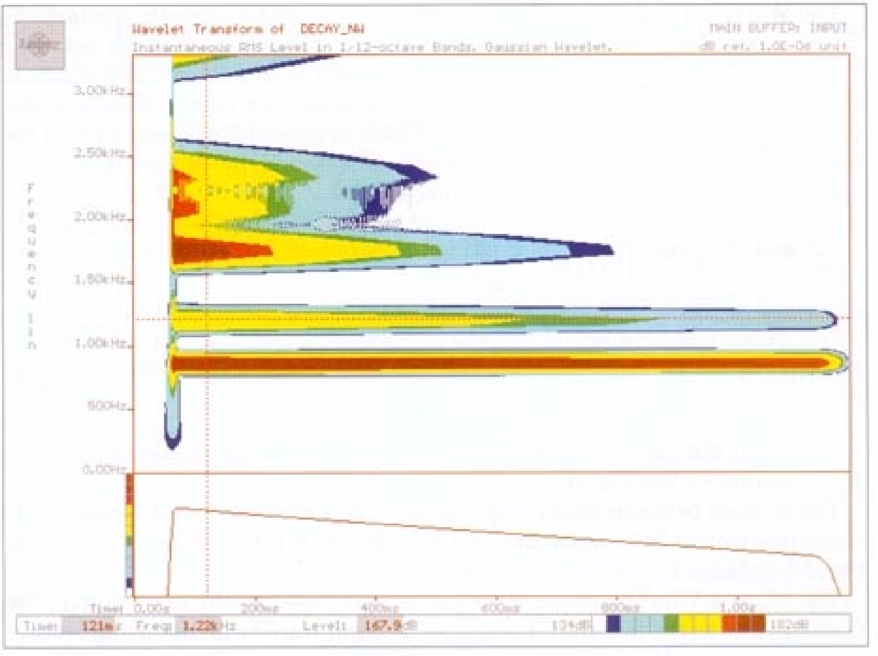

Fig. 21. 1/12th octave Wavelet Transform of a free vibration decay measurement. Notice a linear frequency axis has been selected for easy comparison with the results obtained by the STFT shown in Fig. 22. A slice cursor is used to extract the decay curve of one of the resonances for damping calculation

times be difficult to interpret. On the other hand the WVD, which is a global transformation, is regarded as being the most fundamental of all Time-frequency distributions and is defined as

$$W_s(\tau,f) = \int s\,(t+\tau/2)\; s^*\,(t-\tau/2)e^{-j2\pi ft}\mathrm{dt} \qquad (10)$$

where s is the time signal, τ is the time parameter and f is the frequency parameter. Note that WVD is a kind of combined Fourier Transform and auto-correlation calculation, i.e. autospectrum estimate as a function of time or autocorrelation estimate as a function of frequency. One other drawback of the WVD is that it requires large computational power.

As an example, a 1/12th octave WT was applied to the 32K Time Capture recording of the free vibration decay shown in Fig.9. The Time-frequency con-

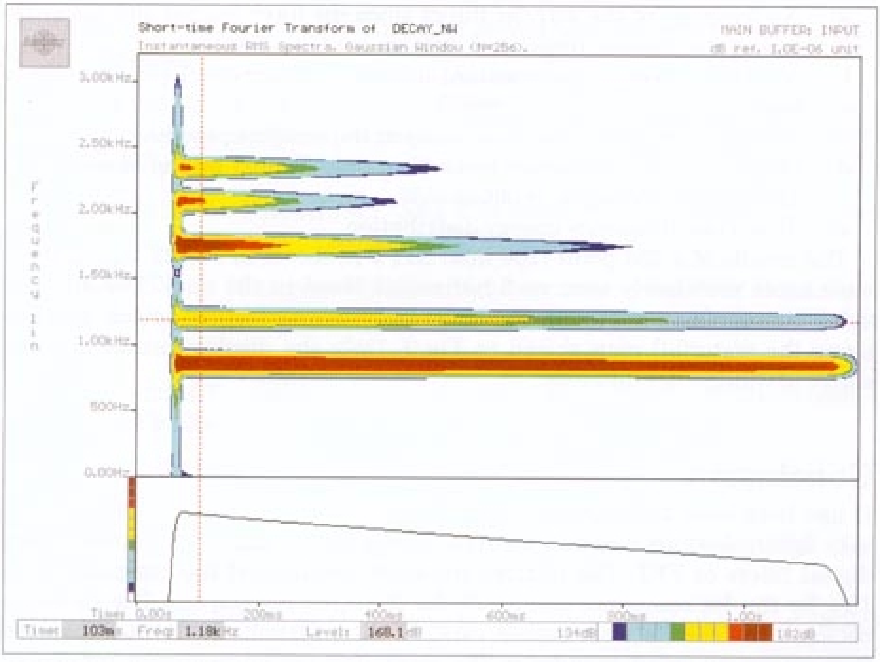

Fig. 22. A 256 point Short-time Fourier Transform of a free vibration decay measurement. A slice cursor is used to extract the decay curve of one of the resonances for damping calculation

tour map is shown in the upper trace of Fig. 21. As a postprocessing possibility the map can be integrated backwards (using the Schroeder method as mentioned earlier) if nescessary.

The 5 resonances are seen as 5 horizontal areas in the map, although the two highest resonances are only separated by two filter bandwidths as seen earlier in Figs. 3 and 5. A slice cursor can be used to extract the levels of a particular resonance frequency as a function of time. This is shown for the second resonance in the lower trace of Fig. 21. Cursor readings confirm the damping results as found earlier.

The main advantages of using fractional octaves Wavelet Transform compared to fractional octaves Digital Filtering for the analysis of non-stationary signals are as follows:

a) No "ringing" of the wavelet filters since the filter shapes and the envelope of the impulse response functions are Gaussian.
b) No RMS detector time-constant limitation, since envelope detection is used.
c) No frequency dependent time delay in the analysis process.
d) Optimum Time-frequency resolution, only limited by the Heisenbergs Uncertainty Principle, is obtainable.
e) True Time-frequency energy distribution.

The results of a 256 point (100 line) STFT is shown in Fig. 22. Again the 5 resonances are clearly seen as 5 horizontal areas in the map. The analysis using contour map shown in Fig. 22 is in practice identical to the analysis using the waterfall map shown in Fig. 9. Only the display format and the choice of window are different.

Conclusion

It has here been demonstrated how damping values of single resonances of very lightly damped structures can be determined by different methods using digital filters or FFT. The relative standard deviation of the estimates were 15% for the 1st resonance and 5-7% for the other resonances. The variation between the results were rather random than systematic. It was observed that extremely small changes in the setup and the environment influenced the damping values up to the observed variances. The use of Time-frequency analysis techniques was also demonstrated.

References

[1] JACOBSEN,F: *"Measurement of structural loss factors by the power input method".* Report No. 41,1986, Acoustics Laboratory of the Danish Technical University

[2] JACOBSEN.F., BAO.D.: *"Acoustic Decay Measurements with a Dual Channel Frequency Analyzer",* Journal of Sound and Vibration (1987) 115(3) pp. 521-537

[3] JACOBSEN.F.: *"A note on Acoustic Decay Measurements",* Journal of Sound and Vibration (1987) 115(1), pp.163-170

[4] JACOBSEN,F., RINDEL,J.H.: Letters to the editor: *"Time Reversed Decay Measurements",* Journal of Sound and Vibration (1987) 117(1), 187-190

[5] JACOBSEN,F.: *"Experimental Determination of Structural Damping",* Proceedings of Nordic Acoustical Meeting, Aalborg, Denmark, 1986, pp. 361-364

[6] CREMER.L., HECKL,M.: *"Structure-Borne Sound",* Berlin, Springer-Verlag, 1973

[7] ZAVERI,K.: *"Complex Modulus Measurements using Wide Band Random Excitation",* Proceedings of Internoise, Beijing, China, 1987, pp. 1383-1386

[8] BROCH,J.T.: *"Mechanical Vibration and Shock Measurements",* Brüel & Kjær, 1980

[9] SCHROEDER.M.R.: *"New Method of Measuring Reverberation Time"* J. Acou. Soc. Am. 37 (1965), pp. 409- 412

[10] HERLUFSEN.H.: *"Dual channel FFT analysis (Part I & II)"* Brüel &Kjaer Technical Review No. 1 & 2,1984

[11] CRAIK, R., NAYLOR, G.: Letters to the editor: *"Measurement of Reverberation Time via Probability Functions"* Journal of Sound and Vibration (1985) 102(3), pp.453-454

[12] GADE.S. & HERLUFSEN,H.: *"Use of Weighting Functions in DFTI FFT analysis",* Brüel & Kjær Technical Reviews Nos. 3 & 4,1987

[13] GRAM-HANSEN, K.: *"Simultaneous Time and Frequency Analysis"* Ph.D. Thesis 1990, The Electronics Institute, Technical University of Denmark

[14] RIOUL.O. & VETTERLI,M.: *"Wavelets and Signal Processing"* IEEE Signal Processing Magazine, October 1991

[15] Brüel&Kjær: *"Non-stationary Signal Analysis Software Type WT9362"* System Development, BU 0152, 1993

[16] HERLUFSEN, H. & GADE, S.: *"Errors Involved in Computing Impulse Response Function via Frequency Response Function".* Mechanical Systems and Signal Processing 6 (3), pp. 193-206,1992

Previously issued numbers of Brüel & Kjær Technical Review

(Continued from cover page 2)

Special technical literature

Brüel & Kjær publishes a variety of technical literature which can be obtained from your local Brüel & Kjær representative.
The following literature is presently available:

○ Modal Analysis of Large Structures-Multiple Exciter Systems (English)
○ Acoustic Noise Measurements (English), 5th. Edition
○ Noise Control (English, French)
○ Frequency Analysis (English), 3rd. Edition
○ Catalogues (several languages)
○ Product Data Sheets (English, German, French, Russian)

Furthermore, back copies of the Technical Review can be supplied as shown in the list above. Older issues may be obtained provided they are still in stock.

Brüel & Kjær

WORLD HEADQUARTERS: DK-2850 Nærum · Denmark
Telephone: +45 42 80 05 00 · Telex: 37316 bruka dk · Fax: +45 42 80 14 05

Australia (02) 450-2066 · Austria 0222/816 74 00 · Belgium 016/44 92 25 · Brazil (011) 246-8149/246-8166
Canada (514) 695-8225 · Czech Republic 02-24 3104 58 · Finland (0) 1481577 · France (1) 64 57 20 10
Germany 04106/70 95-0 · Great Britain (081) 954-2366 · Holland 03402-39994 · Hong Kong 548 7486
Hungary (1) 215 83 05/215 89 29 · Italy (02) 57 60 4141 · Japan 03-5420-7302 · Republic of Korea (02) 554-0605
Norway 66 90 44 10 · Poland (0-22) 40 93 92 · Portugal (1) 65 92 56/65 92 80 · Singapore 225 8533
Slovak Republic 07-55666 · Spain (91) 368 10 00 · Sweden (08) 711 27 30 · Switzerland (1) 862 19 60
Taiwan (02) 713 9303 · Tunisia (01) 232 478 · USA: MA (508) 481-7737 GA (404) 981-6225 MI (313) 522-860
IL (708) 358-7582 CA (714) 978-8066 WA (206) 883-2203/882-4359
Local representatives and service organisations world-wide

ISSN 007 – 2621
BV 0044 – 11

PRINTED IN DENMARK BY NÆRUM OFFSET